Radiative transfer in nonuniformly refracting layered media: atmosphere–ocean system

Zhonghai Jin and Knut Stamnes

We have applied the discrete-ordinate method to solve the radiative-transfer problem pertaining to a system consisting of two strata with different indices of refraction. The refraction and reflection at the interface are taken into account. The relevant changes (as compared with the standard problem with a constant index of refraction throughout the medium) in formulation and solution of the radiative-transfer equation, including the proper application of interface and boundary conditions, are described. Appropriate quadrature points (streams) and weights are chosen for the interface-continuity relations. Examples of radiative transfer in the coupled atmosphere–ocean system are provided. To take into account the region of total reflection in the ocean, additional angular quadrature points are required, compared with those used in the atmosphere and in the refractive region of the ocean that communicates directly with the atmosphere. To verify the model we have tested for energy conservation. We also discuss the effect of the number of streams assigned to the refractive region and the total reflecting region on the convergence. Our results show that the change in the index of refraction between the two strata significantly affects the radiation field. The radiative-transfer model we present is designed for application to the atmosphere–ocean system, but it can be applied to other systems that need to consider the change in the index of refraction between two strata.

1. Introduction

The discrete-ordinate method has been satisfactorily used to solve the radiative-transfer problem in vertically inhomogeneous media. For example, it has been applied to multilayered media with anisotropic scattering,[1] but there has been no need to consider changes in refractive properties because optically only one medium with a constant index of refraction was considered. Today, however, more and more applications in oceanography and climate-change studies have involved two or more subsystems with different indices of refraction. For such situations the change in the index of refraction across the interface between the two media has to be taken into account. Examples are radiative transfer within the atmosphere–ocean system and the atmosphere–sea ice–ocean system.

A number of models, most of them based on the Monte Carlo technique, have been developed and are used for various studies of radiative transfer in the atmosphere ocean system.[2–7] The main purpose of this paper is to extend the discrete-ordinate method, which has proved to be a very efficient method for solving radiative-transfer problems in the atmosphere,[8–10] to a coupled system with a discontinuous interface of the refractive index. The principal difficulty encountered in attempts to model radiative transfer throughout such a system with the discrete-ordinate method originates from the bending or refraction of radiation across the interface between the media of different refractive properties. The Fresnel refraction and reflection will affect the form of the radiative-transfer equation and the particular solutions, and the continuity relations at the interface are totally different from the nonrefractive case. We will take the atmosphere–ocean system as an example and assume a flat air–ocean interface presently. Also, the atmosphere and the ocean are both assumed to be vertically stratified so that the optical properties depend only on the vertical coordinate. To account for the vertical inhomogeneity, the atmosphere and the ocean can be divided into any suitable number of horizontal layers, as required to resolve the vertical structure of the optical properties of each medium.

In the following section, we first derive the formulation of the radiative-transfer equation, which is different from that for the uniformly refracting medium,

The authors are with the Geophysical Institute and the Department of Physics, University of Alaska, Fairbanks, Alaska 99775-0800.

Received 14 January 1993; revised manuscript received 28 May 1993.

0003-6935/94/030431-12$06.00/0.

for a coupled system. We then select an appropriate quadrature and apply the discrete-ordinate method to find a general solution which is suitable for every layer. Finally we discuss the formulation and procedure required to apply the interface and boundary conditions to such a coupled system. In Section 3, some model-consistency tests are performed, the importance of proper stream distributions in the Fresnel cone and the total reflection region in the ocean to achieving fast convergence is discussed, and the effect of scattering asymmetry on convergence is studied. Following that, some results from applying this formalism to the atmosphere–ocean system are presented, including comparisons performed with and without the inclusion of the effects arising from the change in the index of refraction at the air–ocean interface. Those comparisons demonstrate the importance of including this change in the refractive index.

2. Equations and Solutions

Formulation and solution of the radiative-transfer equation for the atmosphere–ocean system have a lot in common with that for the atmosphere only. In this paper we emphasize the differences. Therefore, only solar radiation is considered, because it is strongly affected by the refractive-index change and exhibits a much different transfer process in the coupled system. We will neglect the thermal emission and give the homogeneous solution directly, as it is basically the same as that which is obtained when considering only the atmosphere.

Figure 1 illustrates the radiative-transfer model for the atmosphere–ocean system schematically. In the ocean, region I is the total-reflection region. Region II is the refraction region. The width of each region depends on the relative index of refraction of the two media. The downward radiation distributed over 2π steradians in the atmosphere will be restricted to a cone (less than 2π steradians) after being refracted across the interface into the ocean. Photons in region II of the ocean may be scattered into region I. Note, however, that photons in region I of the ocean cannot reach the atmosphere directly and vice versa. Communication between the atmosphere and region I must occur through the scattering process between region I and region II in the ocean. All these characteristics for the coupled system can be described with a properly formulated radiative-transfer equation and appropriate implementation.

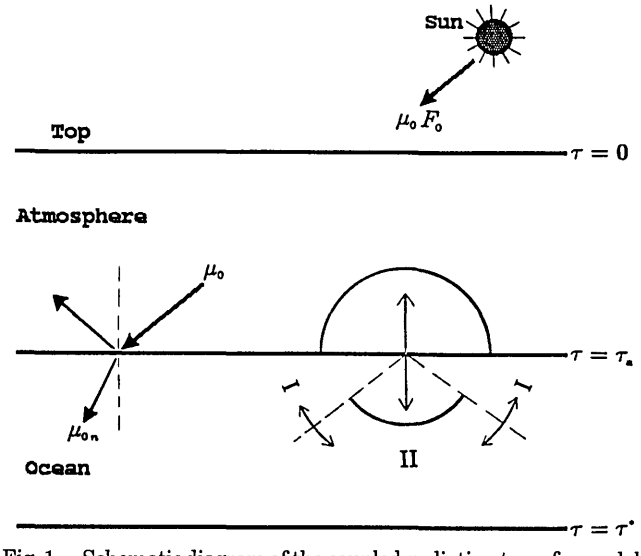

Fig. 1. Schematic diagram of the coupled-radiative-transfer model for the atmosphere–ocean system.

A. Basic Equations

The equation describing the radiation transfer through a plane-parallel medium is given by[9,11]

$$\mu \frac{dI(\tau, \mu, \phi)}{d\tau} = I(\tau, \mu, \phi) - S(\tau, \mu, \phi), \qquad (1)$$

where $I(\tau, \mu, \phi)$ is the specific intensity (radiance) at vertical optical depth τ (measured downward from the upper boundary) in direction (μ, ϕ) (μ is the cosine of the polar angle, which is positive with respect to the upward normal, and ϕ is the azimuthal angle). The source function is

$$S(\tau, \mu, \phi) = \frac{\omega(\tau)}{4\pi} \int_0^{2\pi} d\phi' \int_{-1}^{1} p(\tau, \mu, \phi, \mu', \phi') \times I(\tau, \mu', \phi') d\mu' + Q(\tau, \mu, \phi), \qquad (2)$$

where $\omega(\tau)$ is the single-scattering albedo, $p(\tau, \mu, \phi, \mu', \phi')$ is the phase function, and $Q(\tau, \mu, \phi)$ represents the actual internal source. The solar-beam source in the atmosphere can be expressed as

$$Q_{\text{air}}(\tau, \mu, \phi) = \frac{\omega(\tau)}{4\pi} F_0 p(\tau, \mu, \phi, -\mu_0, \phi_0) \exp(-\tau/\mu_0) + \frac{\omega(\tau)}{4\pi} F_0 R(-\mu_0, n) p(\tau, \mu, \phi, \mu_0, \phi_0) \times \exp[-(2\tau_a - \tau)/\mu_0], \qquad (3)$$

where μ_0 is the cosine of the solar zenith angle and is positive, ϕ_0 is the azimuthal angle for the incident solar beam, and F_0 is the solar-beam intensity at the top of the atmosphere. Here n is the index of refraction of the ocean relative to the atmosphere, and τ_a is the total optical depth of the atmosphere. The first term in Eq. (3) represents the contribution from the downward, incident beam source, while the second term represents the contribution from the upward beam source reflected at the atmosphere–ocean interface because of the Fresnel reflection caused by the change in the refractive index between air and sea water. $R(-\mu_0, n)$ is the ocean-surface reflectance for the solar beam. In the ocean, the source term is

$$Q_{\text{ocn}}(\tau, \mu, \phi) = \frac{\omega(\tau)}{4\pi} \frac{\mu_0}{\mu_{0n}(\mu_0, n)} F_0 T(-\mu_0, n) \times p(\tau, \mu, \phi, -\mu_{0n}, \phi_0) \exp(-\tau_a/\mu_0) \times \exp[-(\tau - \tau_a)/\mu_{0n}], \qquad (4a)$$

where $T(-\mu_0, n)$ is the transmittance through the interface, and μ_{0n} is the cosine of the solar zenith angle in the ocean, which is related to μ_0 by the Snell law:

$$\mu_{0n}(\mu_0, n) = \sqrt{1 - (1 - \mu_0^2)/n^2}. \quad (4b)$$

Expansion of the phase function $p(\tau, \cos\Theta)$ in a series of $2N$ Legendre polynomials and the intensity in a Fourier cosine series[1,11]

$$I(\tau, \mu, \phi) = \sum_{m=0}^{2N-1} I^m(\tau, \mu)\cos m(\phi - \phi_0) \quad (5a)$$

$$p(\tau; \mu, \phi, \mu', \phi') \equiv p(\tau; \cos\Theta) = \sum_{l=0}^{2N-1} (2l + 1)g_l(\tau)P_l(\cos\Theta), \quad (5b)$$

which leads to the replacement of Eq. (1) with $2N$ independent equations (one for each Fourier component):

$$\mu \frac{dI^m(\tau, \mu)}{d\tau} = I^m(\tau, \mu) - \int_{-1}^{1} D^m(\tau, \mu, \mu')I^m(\tau, \mu')d\mu' - Q^m(\tau, \mu), \quad m = 0, 1, \ldots, 2N - 1, \quad (6a)$$

$$D^m(\tau, \mu, \mu') = \frac{\omega(\tau)}{2} \sum_{l=m}^{2N-1} (2l + 1)g_l(\tau) \times \frac{(l - m)!}{(l + m)!} P_l^m(\mu)P_l^m(\mu'), \quad (6b)$$

where Θ is the scattering angle, $P_l^m(\mu)$ is the associated Legendre polynomial, $g_l(\tau)$ is the expansion coefficient, and $Q^m(\tau, \mu)$ is the mth Fourier component of the beam source. In the atmosphere it is

$$Q_{\text{air}}{}^m(\tau, \mu) = X_0{}^m(\tau, \mu)\exp(-\tau/\mu_0) + X_{01}{}^m(\tau, \mu)\exp(\tau/\mu_0), \quad (6c)$$

where

$$X_0{}^m(\tau, \mu) = \frac{\omega(\tau)}{4\pi} F_0(2 - \delta_{m0}) \sum_{l=0}^{2N-1} (-1)^{l+m}(2l + 1)g_l(\tau) \times \frac{(l - m)!}{(l + m)!} P_l^m(\mu)P_l^m(\mu_0), \quad (6d)$$

$$X_{01}{}^m(\tau, \mu) = \frac{\omega(\tau)}{4\pi} F_0 R(-\mu_0, n)\exp(-2\tau_a/\mu_0)(2 - \delta_{m0}) \times \sum_{l=0}^{2N-1} (2l + 1)g_l(\tau) \frac{(l - m)!}{(l + m)!} \times P_l^m(\mu)P_l^m(\mu_0), \quad (6e)$$

$$\delta_{m0} = \begin{cases} 1, & \text{if } m = 0; \\ 0, & \text{otherwise.} \end{cases} \quad (6f)$$

The source term in ocean can be expressed as

$$Q_{\text{ocn}}{}^m(\tau, \mu) = X_{02}{}^m(\tau, \mu)\exp(-\tau/\mu_{0n}), \quad (6g)$$

where

$$X_{02}{}^m(\tau, \mu) = \frac{\omega(\tau)}{4\pi} \frac{\mu_0}{\mu_{0n}(\mu_0, n)} T\left\{(-\mu_0, n)F_0 \exp\left[-\tau_a\left(\frac{1}{\mu_0} - \frac{1}{\mu_{0n}}\right)\right]\right\} \times (2 - \delta_{m0}) \sum_{l=0}^{2N-1} (-1)^{l+m}(2l + 1)g_l(\tau) \times \frac{(l - m)!}{(l + m)!} P_l^m(\mu)P_l^m(\mu_{0n}). \quad (6h)$$

B. Quadrature Rule And Discrete-Ordinate Approximation

The discrete-ordinate approximation to Eq. (6a) is obtained by replacing the integral in Eq. (6a) by a quadrature sum, thus transforming the integrodifferential Eq. (6a) into a system of coupled differential equations. Thus, for each layer in the atmosphere, we obtain[1]

$$\mu_i{}^a \frac{dI^m(\tau, \mu_i{}^a)}{d\tau} = I^m(\tau, \mu_i{}^a) - \sum_{\substack{j=-N_1 \\ j\neq 0}}^{N_1} w_j{}^a D^m(\tau, \mu_i{}^a, \mu_j{}^a) \times I^m(\tau, \mu_j{}^a) - Q_{\text{air}}{}^m(\tau, \mu_i{}^a), \quad i = \pm 1, \ldots, \pm N_1, \quad (7)$$

and similarly, for layers in the ocean, we find

$$\mu_i{}^o \frac{dI^m(\tau, \mu_i{}^o)}{d\tau} = I^m(\tau, \mu_i{}^o) - \sum_{\substack{j=-N_2 \\ j\neq 0}}^{N_2} w_j{}^o D^m(\tau, \mu_i{}^o, \mu_j{}^o) \times I^m(\tau, \mu_j{}^o) - Q_{\text{ocn}}{}^m(\tau, \mu_i{}^o), \quad i = \pm 1, \ldots, \pm N_2, \quad (8)$$

where $\mu_i{}^a$, $w_i{}^a$ and $\mu_i{}^o$, $w_i{}^o$ are quadrature points and weights for the atmosphere and the ocean, respectively, and $\mu_{-i} = -\mu_i$, $w_{-i} = w_i$. Note that instead of using a constant number of streams for each layer as is usual, we have used different numbers of streams for the atmosphere and the ocean ($2N_1$ and $2N_2$, respectively). In region II of the ocean, which communicates directly with the atmosphere, we use the same number of streams ($2N_1$) as in the atmosphere. This properly accounts for the shrinking caused by refraction of the angular domain in the ocean. In region I of the ocean, where total reflection of photons moving in the upward direction occurs at the ocean–atmosphere interface, we invoke additional streams ($2N_2 - 2N_1$) to accommodate the scattering interaction between regions I and II in the ocean. Although there are many options for choice of quadrature, this choice will strongly affect the application of interface-continuity conditions and the accuracy of the solution. The quadrature used here is essentially the same as that adopted by Tanaka and Nakajima.[12] The double

Guass quadrature rule is used to determine the quadrature points and weights, μ_i^a and w_i^a ($i = 1, \ldots, N_1$), in the atmosphere, as well as the quadrature points and weights, μ_i^o and w_i^o ($i = N_1 + 1, \ldots, N_2$), in the total-reflection region of the ocean. The quadrature points in the Fresnel cone of the ocean are obtained by simply refracting the downward streams in the atmosphere ($\mu_1^a, \ldots, \mu_{N_1}^a$), into the ocean.[7,13] Thus, in this region, μ_i^o is related to μ_i^a by the Snell law,

$$\mu_i^o = S(\mu_i^a) = \sqrt{1 - [1 - (\mu_i^a)^2]/n^2}, \quad i = 1, 2, \ldots, N_1, \tag{9}$$

and from this relation, the weights for this region can be derived as

$$w_i^o = w_i^a \left(\frac{dS(\mu^a)}{d\mu^a}\right)_{\mu^a = \mu_i^a} = \frac{\mu_i^a}{n^2 S(\mu_i^a)} w_i^a, \quad i = 1, 2, \ldots, N_1. \tag{10}$$

The advantage of this choice of quadrature is that the points are clustered toward $\mu = 0$ both in the atmosphere and in the ocean, and in addition, toward the critical-angle direction in the ocean. This clustering gives superior results near these directions where the intensities vary rapidly. Also, this choice of quadrature will simplify the application of the interface-continuity condition and avoid the loss of accuracy incurred by the interpolation necessitated by adopting the same quadrature (i.e., the same number of streams) for the atmosphere and the ocean.

Finally, it is easy to show that the chosen quadrature points and weights make phase-function renormalization unnecessary, so that energy conservation is satisfied automatically, as pointed out first by Wiscombe.[14]

C. Solution

An accurate, reliable, and efficient method of obtaining the solution of the homogeneous version of Eqs. (7) or (8) was presented by Stamnes and Swanson.[10] Following the same procedure, we give the homogeneous solution here.[1] In the atmosphere, (omitting hereafter the superscript m denoting the Fourier components), it is

$$I(\tau, \mu_i^a) = \sum_{j=1}^{N_1} [C_{-j} G_{-j}(\mu_i^a) \exp(k_j^a \tau) + C_j G_j(\mu_i^a) \exp(-k_j^a \tau)], \quad i = \pm 1, \ldots, \pm N_1, \tag{11a}$$

and similarly, in the ocean

$$I(\tau, \mu_i^o) = \sum_{j=1}^{N_2} [C_{-j} G_{-j}(\mu_i^o) \exp(k_j^o \tau) + C_j G_j(\mu_i^o) \exp(-k_j^o \tau)], \quad i = \pm 1, \ldots, \pm N_2, \tag{11b}$$

where k_j and G_j are eigenvalues and eigenvectors, respectively, determined by solving an algebraic eigenvalue problem, and C_j and C_{-j} are unknown constants of integration, to be determined by the application of boundary and continuity conditions as discussed below.

As for the particular solution, in the atmosphere it can be expressed as

$$U(\tau, \mu_i^a) = Z_0(\mu_i^a) \exp(-\tau/\mu_0) + Z_{01}(\mu_i^a) \exp(\tau/\mu_0), \tag{12a}$$

where $i = \pm 1, \pm 2, \ldots, \pm N_1$. The coefficients $Z_0(\mu_i^a)$ and $Z_{01}(\mu_i^a)$ are determined by the following system of linear algebraic equations:

$$\sum_{\substack{j=-N_1 \\ j \neq 0}}^{N_1} \left[\left(1 + \frac{\mu_j^a}{\mu_0}\right)\delta_{ij} - w_j^a D(\tau, \mu_i^a, \mu_j^a)\right] Z_0(\mu_j^a) = X_0(\tau, \mu_i^a), \tag{12b}$$

$$\sum_{\substack{j=-N_1 \\ j \neq 0}}^{N_1} \left[\left(1 + \frac{\mu_j^a}{\mu_0}\right)\delta_{ij} - w_j^a D(\tau, \mu_i^a, \mu_j^a)\right] Z_{01}(\mu_j^a) = X_{01}(\tau, \mu_i^a). \tag{12c}$$

The particular solution in the ocean can be expressed as

$$U(\tau, \mu_i^o) = Z_{02}(\mu_i^o) \exp[-\tau/\mu_{0n}(\mu_0, n)], \tag{13a}$$

where $i = \pm 1, \pm 2, \ldots, \pm N_2$, and $Z_{02}(\mu_i^o)$ is determined by the following system of linear algebraic equations:

$$\sum_{\substack{j=-N_2 \\ j \neq 0}}^{N_2} \left[\left(1 + \frac{\mu_j^o}{\mu_{0n}}\right)\delta_{ij} - w_j^o D(\tau, \mu_i^o, \mu_j^o)\right] Z_{02}(\mu_j^o) = X_{02}(\tau, \mu_i^o). \tag{13b}$$

The general solution is just the sum of the homogeneous solution and the particular solution.

D. Conditions for Boundary, Continuity, and Atmosphere–Ocean Interfaces

The vertically inhomogeneous medium is represented by multiple, adjacent homogeneous layers in the atmosphere and the ocean, respectively. The solutions derived previously will be used in each layer. We assume that the system consists of L_1 layers of atmosphere and L_2 layers of ocean. Then we may write the solution for the pth layer as

$$I_p(\tau, \mu_i^a) = \sum_{j=1}^{N_1} [C_{-jp} G_{-jp}(\mu_i^a) \exp(k_{jp}^a \tau) + C_{jp} G_{jp}(\mu_i^a) \exp(-k_{jp}^a \tau)] + U_p(\tau, \mu_i^a), \quad i = \pm 1, \ldots, \pm N_1 \text{ and } p \leq L_1, \tag{14}$$

$$I_p(\tau, \mu_i^o) = \sum_{j=1}^{N_2} [C_{-jp} G_{-jp}(\mu_i^o) \exp(k_{jp}^o \tau) + C_{jp} G_{jp}(\mu_i^o) \exp(-k_{jp}^o \tau)] + U_p(\tau, \mu_i^o),$$
$$i = \pm 1, \ldots, \pm N_2 \text{ and } L_1 < p \leq L_1 + L_2. \quad (15)$$

There are $2N_1 \times L_1 + 2N_2 \times L_2$ unknown coefficients C_{jp} in Eqs. (14) and (15). They are determined by three factors: the boundary conditions to be applied at the top of the atmosphere and the bottom of the ocean; the continuity conditions at each interface between layers in the atmosphere and ocean; and finally the reflection and refraction occurring at the atmosphere–ocean interface, where we require Fresnel's equations to be satisfied.

These conditions are implemented as follows: At the top we require

$$I_1(0, -\mu_i^a) = I_\infty(-\mu_i^a), \quad i = 1, \ldots, N_1, \quad (16a)$$

at the interfaces between atmospheric layers we require

$$I_p(\tau_p, \mu_i^a) = I_{p+1}(\tau_p, \mu_i^a), \quad i = \pm 1, \ldots, \pm N_1, \text{ and } p = 1, \ldots, L_1 - 1; \quad (16b)$$

at the interface between the atmosphere and the ocean we require

$$I_{L_1}(\tau_a, \mu_i^a) = I_{L_1}(\tau_a, -\mu_i^a) R(-\mu_i^a, n) + [I_{L_1+1}(\tau_a, \mu_i^o)/n^2] T(+\mu_i^o, n), \quad i = 1, 2, \ldots, N_1, \quad (16c)$$

$$I_{L_1+1}(\tau_a, -\mu_i^o)/n^2 = [I_{L_1+1}(\tau_a, \mu_i^o)/n^2] R(+\mu_i^o, n) + I_{L_1}(\tau_a, -\mu_i^a) T(-\mu_i^a, n), \quad i = 1, 2, \ldots, N_1, \quad (16d)$$

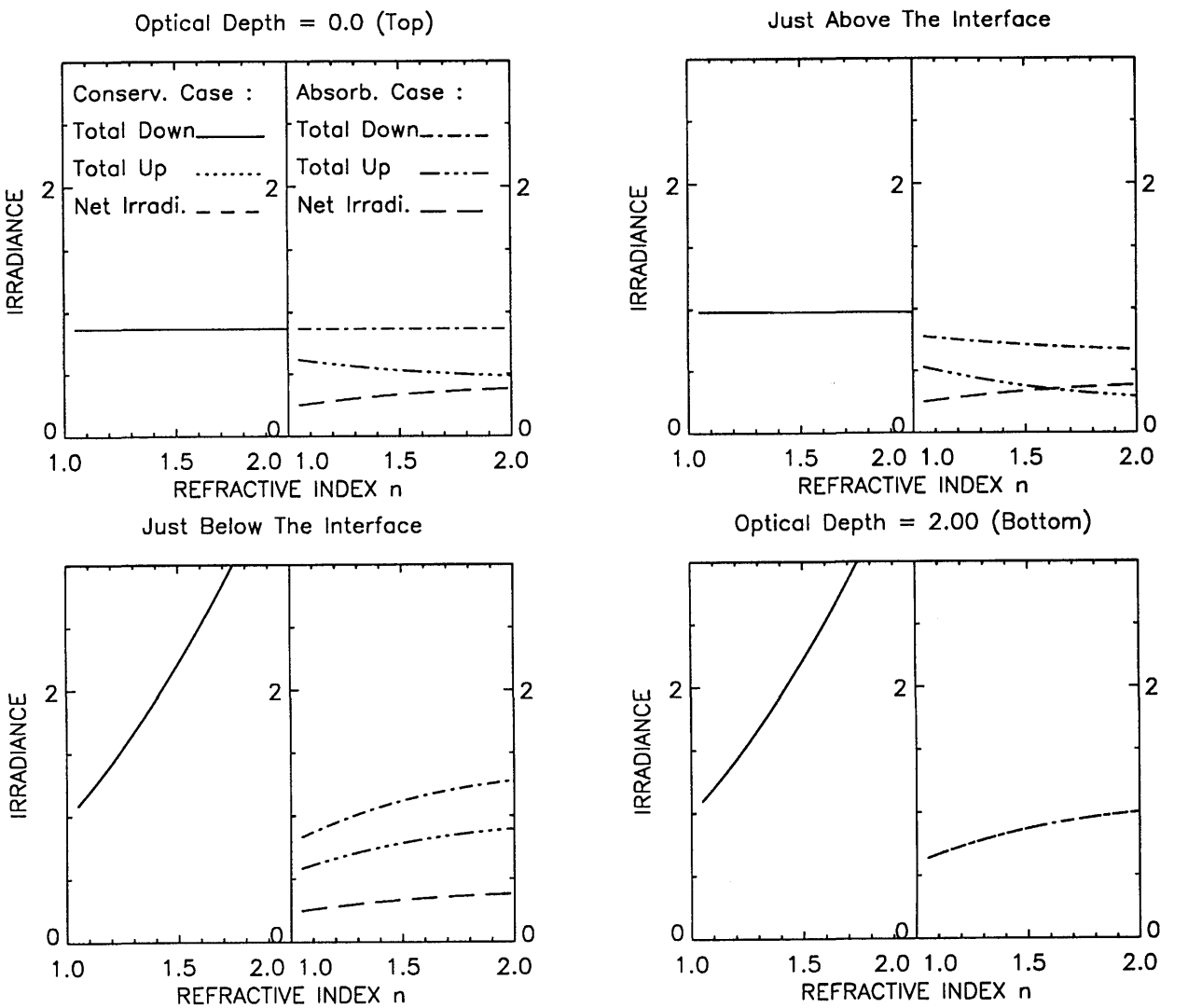

Fig. 2. Variation of irradiances with the relative index of refraction at several locations for isotropic scattering, incident flux $F_0 = 1.0$, with incident zenith angle $\theta_0 = 30°$, bottom-surface albedo = 1.0, $\tau_a = 1.0$, and $\tau^* = 2.0$. For the absorption case, the only difference from the conserevative case is in the single-scattering albedo, $\omega = 0.9$, in the lower medium.

$$I_{L_1+1}(\tau_a, -\mu_i^o) = I_{L_1+1}(\tau_a, \mu_i^o),$$
$$i = N_1 + 1, \ldots, N_2; \qquad (16e)$$

at the interfaces between ocean layers we require

$$I_p(\tau_p, \mu_i^o) = I_{p+1}(\tau_p, \mu_i^o),$$
$$i = \pm 1, \ldots, \pm N_2, \qquad p = L_1 + 1, \ldots, L_1 + L_2 - 1; \qquad (16f)$$

and finally at the bottom boundary we require

$$I_{L_1+L_2}(\tau^*, \mu_i^o) = I_g(\mu_i^o), \qquad i = 1, 2, \ldots, N_2. \qquad (16g)$$

We define $R(\pm\mu_i, n)$ and $T(\pm\mu_i, n)$ as the specular reflectance and transmittance, respectively, of the invariant intensity I/n_{abs}^2, where n_{abs} is the absolute index of refraction at the location where I is measured. The minus sign applies for the downward intensity, and the positive sign for the upward intensity. Formulas for R and T can be derived from the basic Fresnel equations. The results are

$$R(-\mu_i^a, n) = \frac{1}{2}\left[\left(\frac{\mu_i^a - n\mu_i^o}{\mu_i^a + n\mu_i^o}\right)^2 + \left(\frac{\mu_i^o - n\mu_i^a}{\mu_i^o + n\mu_i^a}\right)^2\right], \qquad (17a)$$

$$R(+\mu_i^o, n) = R(-\mu_i^a, n), \qquad (17b)$$

$$T(-\mu_i^a, n) = 2n\mu_i^a\mu_i^o\left[\left(\frac{1}{\mu_i^a + n\mu_i^o}\right)^2 + \left(\frac{1}{\mu_i^o + n\mu_i^a}\right)^2\right] \qquad (17c)$$

$$T(+\mu_i^o, n) = T(-\mu_i^a, n). \qquad (17d)$$

Equations (16c) and (16d) ensure that, by satisfying Fresnel's equations, the radiation fields in the atmosphere and the ocean are properly coupled through the interface, whereas Eq. (16e) represents the total

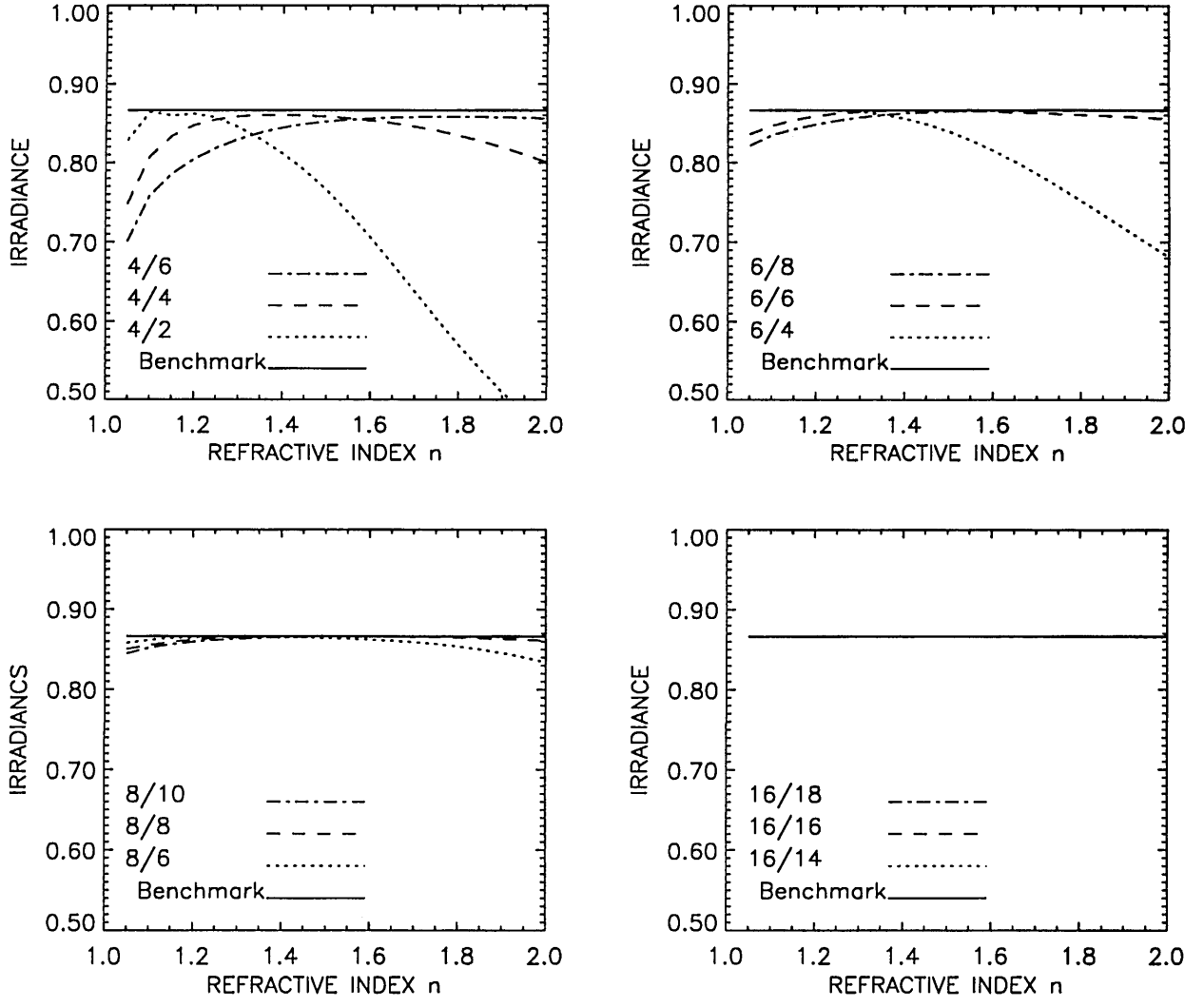

Fig. 3. The effect of stream combinations within the refractive region and the total reflective region (represented by the number ratio) on the convergence for the Henyey–Greenstein scattering-phase function, with asymmetry factor $g = 0.7$. Other input parameters are the same as those for the conservative case in Fig. 2. Shown in the panels are the upward irradiances at the tops of the slabs and their comparison with the Benchmark irradiance incident on the system.

reflection in region I in the ocean. The total optical depth of the atmosphere and ocean is denoted by τ^* in Eq. (16g). $I_\infty(-\mu_i^a)$ is the intensity incident at the top of the atmosphere, and $I_g(\mu_i^o)$ is determined by the bidirectional reflectance of the underlying surface at the bottom of the ocean.[1] Substitution of Eqs. (14) and (15) into Eqs. (16a)–(16g) leads to a system of $2N_1 \times L_1 + 2N_2 \times L_2$ linear algebraic equations for the same number of unknown coefficients, the $C_{\pm jp}$. Matrix inversion of this system of equations yields the desired coefficients and thereby completes the solution for the coupled atmosphere–ocean system. Once we have obtained the solutions for each (and all) Fourier components using Eqs. (14) and (15), we may compute the intensity (radiance) at the quadrature directions from Eq. (5). Irradiances (fluxes) and mean intensity can now be easily computed from the zero-order Fourier component of the intensity given above by using the same quadrature rule to convert integrals into simple summations.[9]

3. Some Results and Discussion

A. Model Test

Before considering an actual application, we shall discuss a number of consistency and convergence tests aimed at checking the basic soundness of the solution. First we consider a conservative situation, in which case there is no absorption at all in the whole system. In another words, we replace the atmosphere and the ocean with two strata consisting of media with different refractive indices, but without absorption. At the bottom of the lower stratum, we assume that the surface is totally reflecting. The variation in irradiances with the relative index of refraction n at four particular levels is shown in Fig. 2. The effect of adding some absorption is also illustrated. The net irradiance is defined as the difference between the total downward irradiance and the total upward irradiance. In the conservative case, the net irradiance is zero everywhere, consistent with the energy-conservation requirement, so that

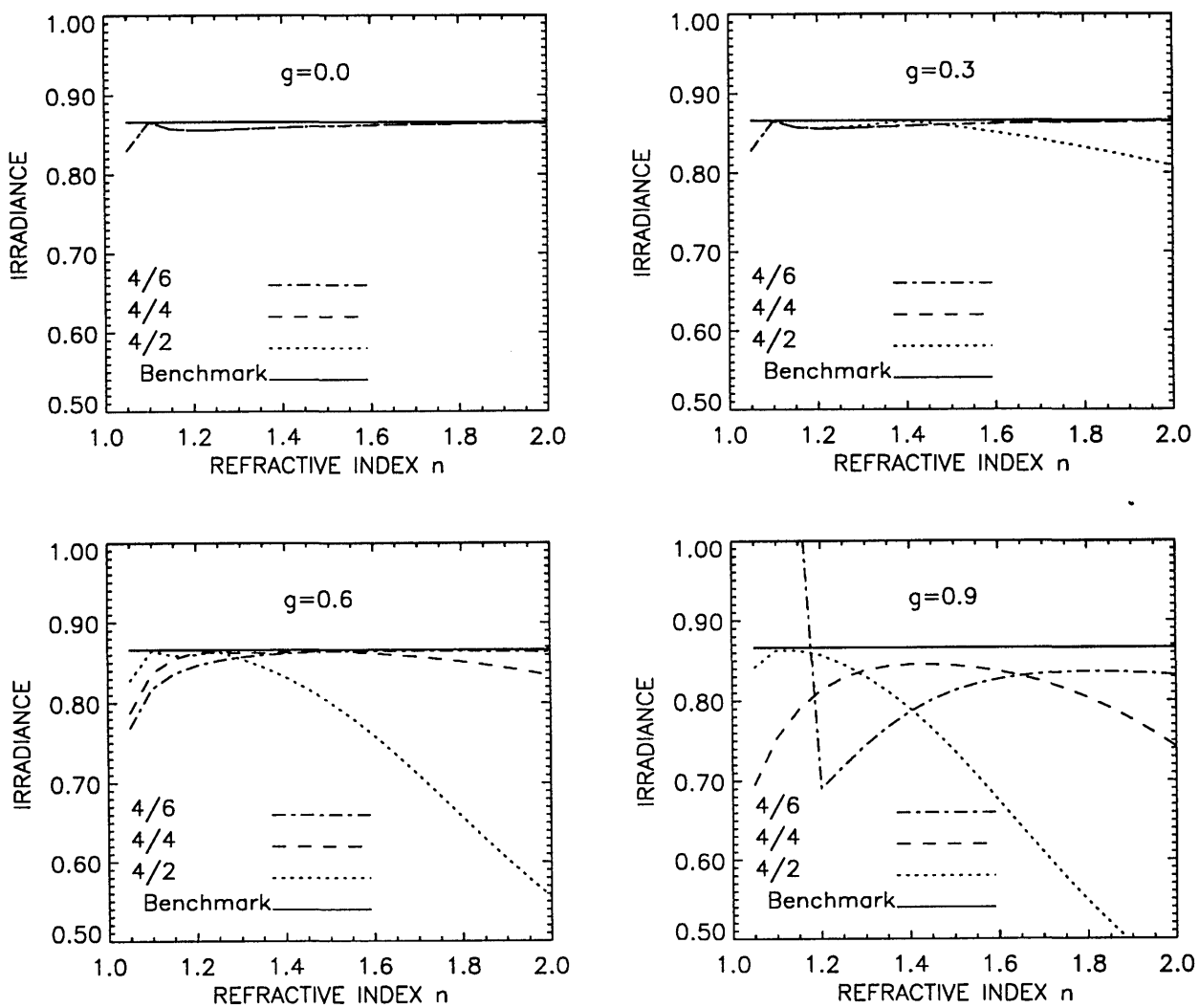

Fig. 4. Similar to Fig. 3 but showing the effect of scattering asymmetry on the irradiance computation (for only one group of stream combinations).

the total upward irradiance overlaps with the total downward irradiance everywhere. The total downward and upward irradiances increase rapidly with increasing n in the lower stratum, but not in the upper stratum because of energy trapping, as discussed by Stavn *et al.*[15] and by Plass *et al.*[13] Figure 2 also shows that the variation in the irradiances with n is very sensitive to the absorption in the lower medium. A single-scattering albedo of 0.9 in just the lower medium leads to a drastic reduction of the irradiance changes versus n, as compared with the conservative case. At the bottom, the total upward irradiance overlaps with the total downward irradiance for this absorptive case and owes to the assumed bottom-surface albedo of unity. The results shown in Fig. 2 pertain to isotropic scattering, but we have verified by computations that the choice of phase function and optical depth does not significantly affect the general behavior of the irradiances indicated above, for the case of an absorbing lower medium, and there is no effect for the conservative case.

As just discussed, in the conservative case with a surface albedo of unity, the upward irradiance should equal the total downward irradiance at the top. This suggests that for the conservative case, the incident downward irradiance, which is equivalent to $\mu_0 F_0$, can be taken as a benchmark for the total-upward-irradiance computation at the top. Figure 3 shows the computed upward irradiances at the top by using different streams and their comparison with the benchmark with the same conditions as in Fig. 2, but with an asymmetry factor of 0.7 for the Henyey–Greenstein phase function used here. The number ratio represents $2N_1/(2N_2 - 2N_1)$, the number of streams adopted within the refractive region divided by those adopted for the total reflective region. The results indicate that although an increase in the number of streams will eventually increase the accuracy, the convergence speed depends strongly on n for a given combination of streams in the two regions. For example, the upper left panel of Fig. 3 indicates that the combination of 4/2 (four streams for region II and two streams for region I) will produce the best accuracy for smaller values of n (approximately 1.1 to 1.2). The combination of 4/4 is best for n between 1.3 and 1.5, while the combination of 4/6 is better for larger n. Furthermore, as demonstrated in the other three panels, when the number of streams is increased in both regions, the overall accuracy increases as it should. Our computations also show that the convergence behavior indicated above is true at any level. Generally, for larger n, to obtain optimal results we need to assign more streams to the total reflective region because it becomes wider. The quantitative relation between this optimum stream ratio and n is unknown.

In addition to the distribution of quadrature points between the two regions, the convergence speed is also strongly dependent on the asymmetry of the phase function. For the Henyey–Greenstein phase function, which depends only on the asymmetry factor g, Fig. 4 shows that for smaller asymmetry factors (i.e., less anisotropy), fewer quadrature points are needed to attain good accuracy. We have adopted the delta-M transformation,[12] which has been shown to optimize the performance of the model and to improve the accuracy for strongly forward-peaked scattering.

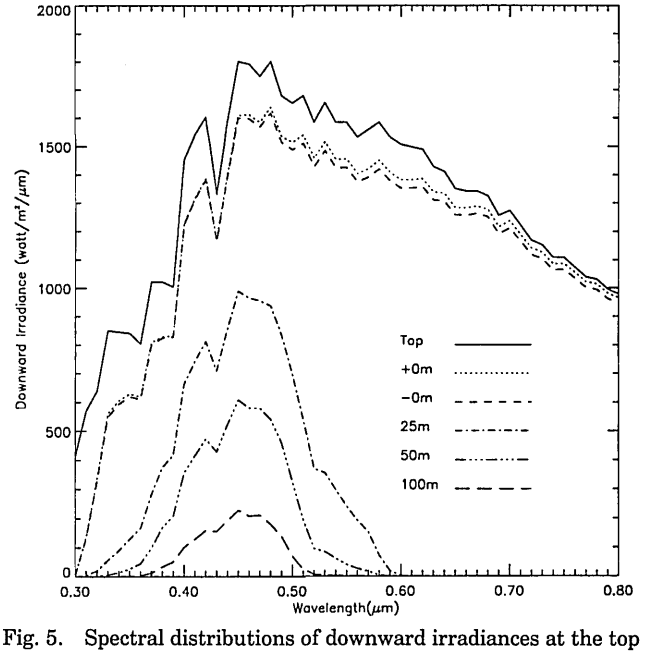

Fig. 5. Spectral distributions of downward irradiances at the top of the atmosphere, just above the ocean surface (+0 m), just below the ocean surface (−0 m), and at several depths in the ocean for a model of a clear midlatitude atmosphere and pure sea water, with a solar zenith angle $\theta_0 = 30°$.

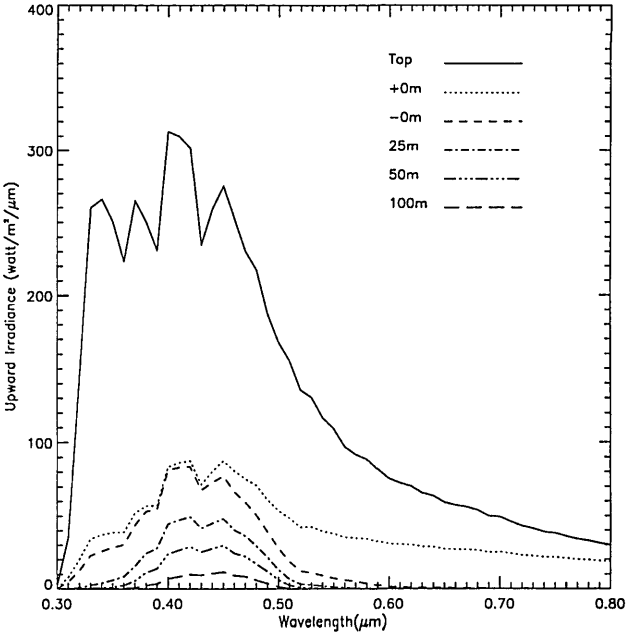

Fig. 6. Similar to Fig. 5 but showing the upward irradiances.

B. Application for the Atmosphere–Ocean System

The comprehensive model described above was applied to the atmosphere–ocean system. We adopted the profile of the midlatitude summer atmosphere developed by McClatchey *et al.*[16] and divided the atmosphere into 24 layers. For simplicity, only pure atmosphere and pure sea water are considered here. Therefore, we may adopt the Rayleigh scattering-phase function for both the atmosphere and the ocean. The optical properties of the clearest ocean water are taken from Smith and Baker.[17] Because of the homogeneity of pure sea water, it is not necessary to use multiple layers in the ocean even though our model can easily accommodate an arbitrary number of layers in the ocean. By assuming a solar zenith angle of 30° and a relative refractive index for the ocean of 1.33 (neglecting for simplicity the wavelength dependence here), we computed downward and upward irradiances at the top of atmosphere, just above and just below the ocean surface, as well as at several depths in the ocean, as shown in Figs. 5 and 6.

In Fig. 7 we show the computed reflectance of the ocean surface for several solar zenith angles and compare it with the result obtained when the effects of refraction are ignored. The differences in the upward and downward irradiances at the ocean surface for having included and neglected refraction are also shown. The results indicate that underestimation of the reflectance would occur for most wavelengths if the change in index of refraction across the interface between the ocean and the atmosphere is ignored. As the solar zenith angle increases, the specular reflection, caused by the difference in the indices of refraction between the atmosphere and the

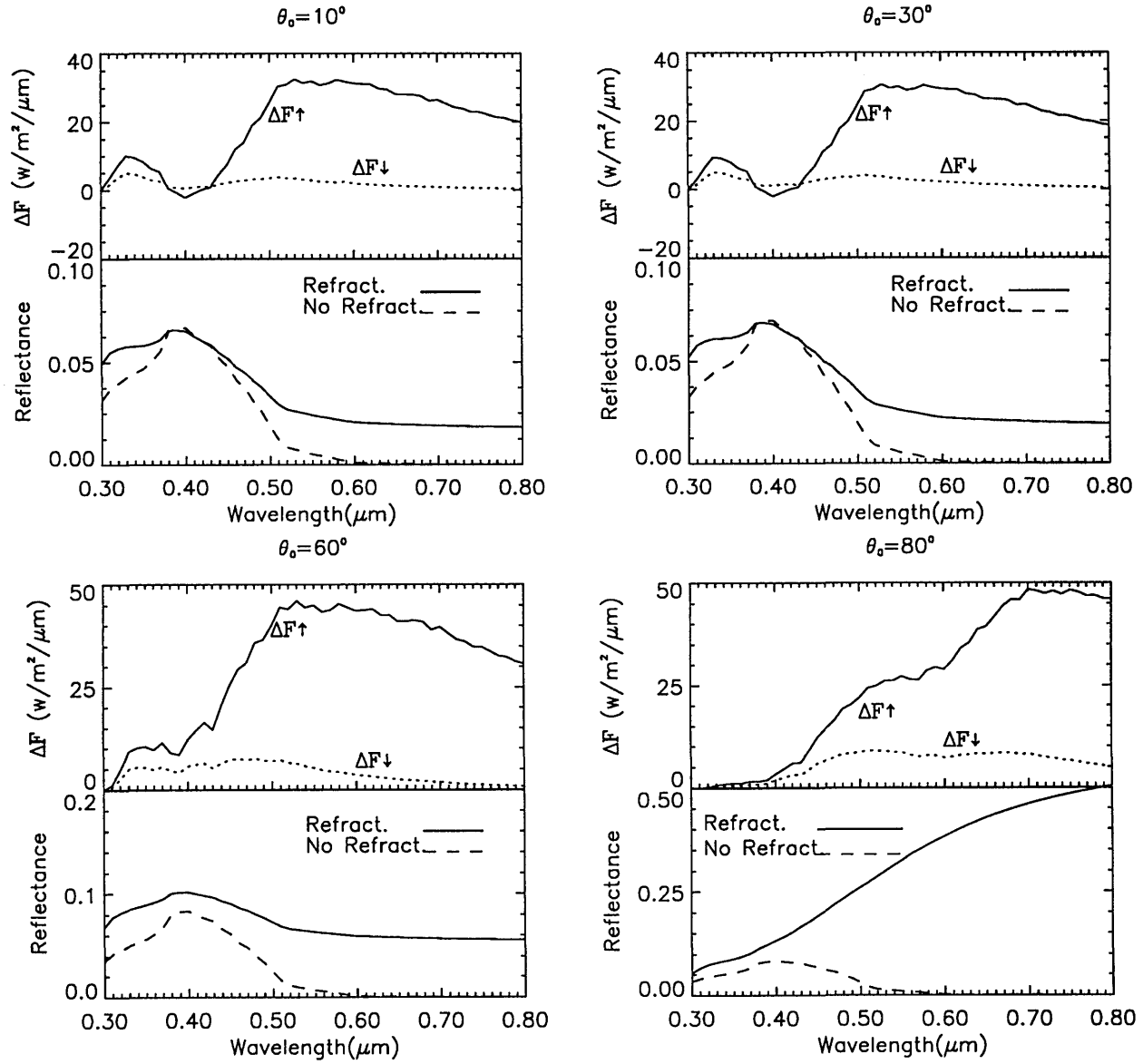

Fig. 7. Spectral distribution of ocean-surface reflectance for considering refraction and neglecting refraction, and for several solar zenith angles. Also shown are the downward and upward irradiance differences at the ocean surface when refraction is considered and neglected, $\Delta F_{\downarrow} = F_{\mathrm{Refr}\downarrow} - F_{\mathrm{Noref}\downarrow}$, $\Delta F_{\uparrow} = F_{\mathrm{Refr}\uparrow} - F_{\mathrm{Noref}\uparrow}$. The same atmospheric and oceanic models used in Fig. 5 are used here.

ocean, contributes more to the total reflectance of the ocean surface, and consequetly more to the upward irradiance at the ocean surface. Therefore, for larger solar zenith angles, the discrepancy between the reflectance computed with and without refraction becomes larger.

Figure 8 shows the distribution of downward irradiance and upward irradiance with height in the atmosphere and with depth in ocean for the same atmosphere and ocean model used above and for a wavelength of 500 nm. For comparison, corresponding results obtained by neglecting the refraction are also displayed. There is considerable interest in energy absorption as a function of altitude in the atmosphere or of depth in the ocean, because this absorbed energy drives the atmospheric and oceanic circulation. Because the absorbed energy within each layer is proportional to the mean intensity (the same as the total scalar irradiance, defined by Morel and Smith,[18] divided by 4π) in that layer, we show in Fig. 9 the mean intensity versus both the height in the atmosphere and the depth in the ocean. Also shown are the same results obtained by ignoring refraction and the relative error, $|(I_{\text{refr}} - I_{\text{norefr}})/I_{\text{refr}}| \times 100$. We note that the relative error may increase up to 20% just below the ocean surface. Although the radiation field is large in the deep ocean, it is already significantly attenuated there.

Figure 10 shows the azimuthally averaged intensity distribution just above and just below the ocean

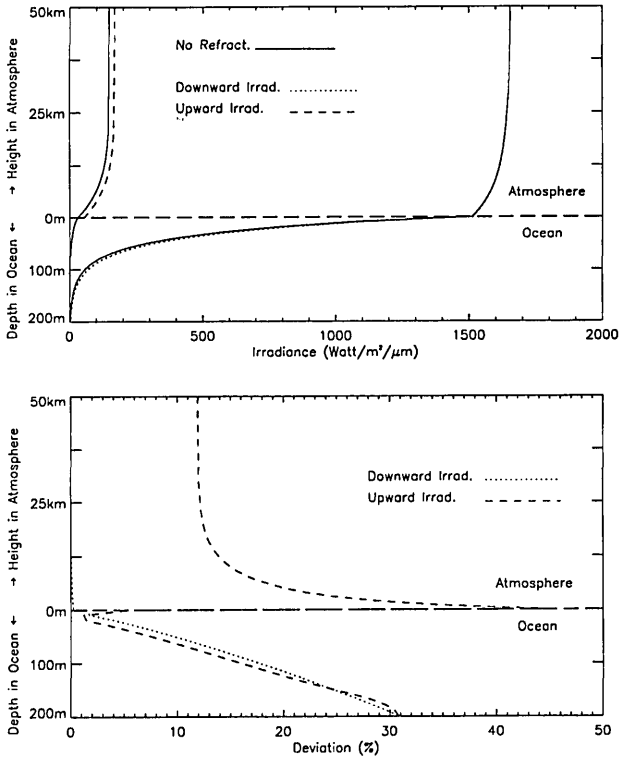

Fig. 8. Distributions of the downward and the upward irradiances with height in the atmosphere and depth in the ocean, the results of neglecting refraction, and the relative deviation. $\theta_0 = 30°$, $\lambda = 500$ nm.

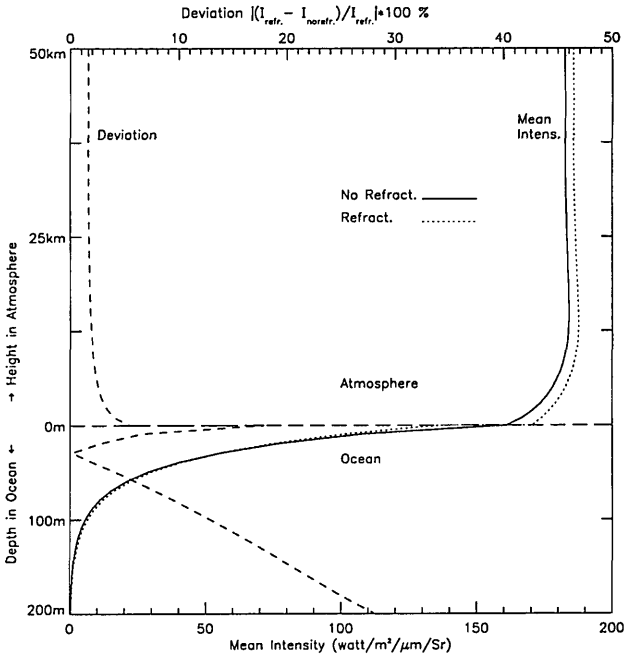

Fig. 9. Distributions of the total mean intensity (total scalar irradiance/4π) with height in the atmosphere and depth in the ocean, the result of neglecting refraction, and the relative deviation. $\theta_0 = 30°$, $\lambda = 500$ nm.

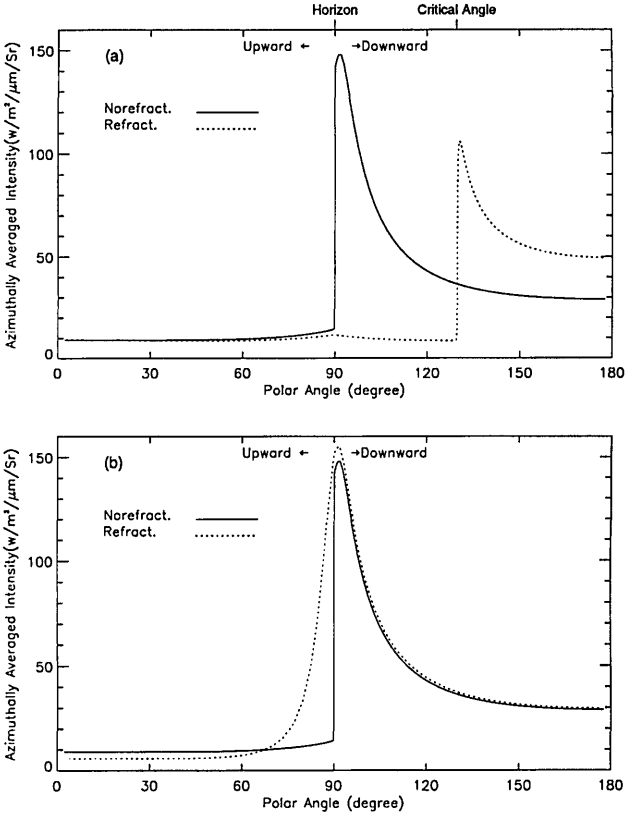

Fig. 10. Distributions of the azimuthally averaged intensity (radiance) for the refraction case ($n = 1.33$) and the no-refraction case ($n = 1.0$); $\theta_0 = 30°$; $\lambda = 500$ nm. (a) Just below the ocean surface, (b) just above the ocean surface.

interface. Again results obtained by ignoring refraction are also displayed. The results indicate that the refraction significantly alters the radiative-intensity distribution. Just below the ocean surface, the downward-intensity discontinuity position shifts from the horizontal direction for the case of no refraction, to the critical-angle direction when refraction is included. The refraction also significantly changes the upward radiation field just above the ocean surface. Knowledge of the intensity distribution here is important for correct interpretations of intensity measurements in remote-sensing applications.

All of the quantities computed above for Figs. 5–10 are calculated to be accurate to within 1%. To achieve this accuracy, a stream ratio of 6/10 (6 streams in the atmosphere, 10 streams in the ocean) was applied in the calculations for Figs. 5–9, while a ratio of 40/70 is used for Fig. 10, but only for the purpose of providing enough points to plot a smoother curve.

The present model has recently been compared with six other models that have approached the radiative-transfer problem in the atmosphere–ocean system with different methods.[19] A typical oceanic phase function with strongly forward scattering was adopted there. Our results calculated with the delta-*M* transformation agreed very well with the results from the other models. The computer resources required for calculation among the models were also compared, showing that our model is especially efficient for the computations of irradiances and azimuthally averaged radiances.

4. Conclusion

We have developed a comprehensive methodology, based on the discrete-ordinate method, for solving the radiative-transfer equation pertinent for a system consisting of two strata with different indices of refraction. The method is well suited to providing consistent solutions of the radiative-transfer problem for the coupled atmosphere–ocean system. The refraction and total reflection at the interface of the two strata have been taken into account by assigning different numbers of angular quadrature points (discrete ordinates or streams) in the atmosphere and the ocean. Thus the interpolation at the interface of two media is entirely avoided, and the radiation field in both the atmosphere and the ocean can be efficiently solved at once. The vertical inhomogeneity of the atmosphere and the ocean can be accounted for by dividing each stratum into a suitable number of homogeneous layers so that the optical properties may be regarded as constant within each layer, but are permitted to vary from layer to layer.

Test results show that the solution conserves energy and is both reliable and efficient. The accuracy depends on the number of streams utilized to make the angular dependence discrete. Good accuracy for irradiance and mean intensity are obtained with just a few streams. Preliminary results of the application to the pure atmosphere–ocean system show that the refraction significantly affects the radiation field and radiative-energy absorption in both the atmosphere and the ocean. A more realistic quantification of the radiation field in the atmosphere and ocean environments can be simulated when actual optical properties of the atmosphere, including clouds and aerosols, and of the ocean, including particulates, versus depth are available. The radiative-transfer model presented in this paper provides a means for estimating light reflection and transmission, as well as rates of warming and cooling, and for studying the radiative interaction between the atmosphere and the ocean. The model could, if so desired, be extended to deal with changes in the index of refraction between all layers instead of just the atmosphere–ocean interface. Such an extension would make it feasible to study radiative transfer within media in which the index of refraction changes continuously throughout the medium. Possible future extensions of the discrete-ordinate method presented here include (1) the simulation of ocean-surface roughness, (2) the computation of inelastic-scattering effects to treat phenomena such as Raman scattering, and (3) the consideration of polarization.

Z. Jin thanks Fé Seymour for help with the English language. This work was supported by the National Science Foundation through grant DPP92–00747 and the Department of Energy through contract 091574–A–Q1.

References

1. K. Stamnes, S. C. Tsay, W. Wiscombe, and K. Jayaweera, "Numerically stable algorithm for discrete-ordinate-method radiative transfer in multiple scattering and emitting layered media," Appl. Opt. **27,** 2502–2509 (1988).
2. C. Mobley, "A numerical model for the computation of radiance distributions in natural waters with wind-roughened surfaces," Limnol. Oceanogr. **34,** 1473–1483 (1989).
3. H. Gordon and M. Wang, "Surface-roughness considerations for atmospheric correction of ocean color sensor. I: The Rayleigh-scattering component," Appl. Opt. **31,** 4247–4260 (1992).
4. G. Kattawar and C. Adams, "Stokes vector calculations of the submarine light field in an atmosphere–ocean with scattering according to a Rayleigh phase matrix: effect of interface refractive index on radiance and polarization," Limnol. Oceanogr. **34,** 1453–1472 (1989).
5. A. Morel and B. Gentili, "Diffuse reflectance of oceanic waters: its dependence on Sun angle as influenced by the molecular-scattering contribution," Appl. Opt. **30,** 4427–4438 (1991).
6. J. Kirk, "Monte Carlo procedure for simulating the penetration of light into natural waters," Division of Plant Industry Tech. Paper 36 (Commonwealth Scientific and Industrial Research Organization, Canberra, Australia, 1981), p. 16.
7. T. Nakajima and M. Tananka, "Effect of wind-generated waves on the transfer of solar radiation in the atmosphere–ocean system," J. Quant. Spectrosc. Radiat. Transfer **29,** 521–537 (1983).
8. S. C. Tsay, K. Stamnes, and K. Jayaweera, "Radiative transfer in stratified atmospheres: development and verification of a unified model," J. Quant. Spectrosc. Radiat. Transfer **43,** 133–148 (1990).

9. K. Stamnes, "The theory of multiple scattering of radiation in plane-parallel atmospheres," Rev. Geophys. **24,** 299–310 (1986).
10. K. Stamnes and R. A. Swanson, "A new look at the discrete-ordinate method for radiative-transfer calculations in anisotropically scattering atmospheres," J. Atmos. Sci. **38,** 387–399 (1981).
11. S. Chandrasekhar, *Radiative Transfer* (Dover, New York, 1960) p. 12.
12. M. Tanaka and T. Nakajima, "Effects of oceanic turbidity and index of refraction of hydrosols on the flux of solar radiation in the atmosphere–ocean system," J. Quant. Spectrosc. Radiat. Transfer **18,** 93–111 (1977).
13. G. Plass, T. Humphreys, and G. Kattawar, "Ocean–atmosphere interface: its influence on radiation," Appl. Opt. **20,** 917–931 (1981).
14. W. J. Wiscombe, "The delta-*M* method: rapid yet accurate radiative-flux calculations for strongly asymmetric phase functions," J. Atmos. Sci. **34,** 1408–1422 (1977).
15. R. Stavn, R. Schiebe, and C. Gallegos, "Optical controls on the radiant-energy dynamics of the air/water interface: the average cosine and the absorption coefficient," in *Ocean Optics VII,* M. A. Blizard, ed., Proc. Soc. Photo-Opt. Instrum. Eng. **489,** 62–67 (1984).
16. R. A. McClatchey, R. W. Fenn, J. E. A. Selby, F. E. Volz, and J. S. Garing, Rep. AFCRL–72–0497, (Air Force Cambridge Research Laboratories, Bedford, Mass., 1972).
17. R. C. Smith and K. S. Baker, "Optical properties of the clearest natural waters," Appl. Opt. **20,** 177–184 (1981).
18. A. Morel and R. C. Smith, "Terminology and units in optical oceanography," Mar. Geol. **5,** 335–349 (1982).
19. C. Mobley, B. Gentili, H. Gordon, Z. Jin, G. Kattawar, A Morel, P. Reinersman, K. Stamnes, and R. Stavn, "Comparison of numerical models for computing underwater light fields," Appl. Opt. (to be published).